Insect Systematics and Diversity, 2025, **9**(5), ixaf035
DOI: https://doi.org/10.1093/isd/ixaf035
Research

ENTOMOLOGICAL SOCIETY OF AMERICA
SHARING INSECT SCIENCE GLOBALLY

OXFORD

Molecular Phylogenetics, Phylogenomics, and Phylogeography

A phylogenomic overview of the ant genus *Tapinoma* Foerster, 1850 (Formicidae: Dolichoderinae), with the phylogeographic history of the ghost ant *Tapinoma melanocephalum*

Oscar Pérez-Flores[1,2], Michael G. Branstetter[3], John T. Longino[4], Pável Matos-Maraví[5], Michaela Borovanska[5], and Milan Janda[1,5,6,*]

[1]Laboratorio Nacional de Análisis y Síntesis Ecológica, Escuela Nacional de Estudios Superiores, Universidad Nacional Autónoma de México, Morelia, Mexico
[2]Posgrado en Ciencias Biológicas, Universidad Nacional Autónoma de México, Mexico City, Mexico
[3]U.S. Department of Agriculture, Agricultural Research Service (USDA-ARS), Pollinating Insects Research Unit, Utah State University, Logan, UT, USA
[4]Department of Biology, University of Utah, Salt Lake City, UT, USA
[5]Biology Centre CAS, Institute of Entomology, Ceske Budejovice, Czech Republic
[6]Faculty of Science, Department of Zoology, Palacky University, Olomouc, Czech Republic

*Corresponding author. Universidad Nacional Autónoma de México, ENES Morelia, Antigua Carretera a Pátzcuaro 8701, Morelia, Michoacán 58190, Mexico (Email: janda@entu.cas.cz).

Subject Editor: Heather Hines

The ant genus *Tapinoma* Foerster, 1850 is a moderately diverse group (81 valid species) that occurs worldwide. It includes the tramp species *T. melanocephalum*, whose evolutionary history, biogeographic origin, and population limits remain unclear. Here, we present a time-calibrated phylogeny and a biogeographic history inference of the genus based on thousands of Ultraconserved Element (UCE) loci. Focusing on *T. melanocephalum*, we used single nucleotide polymorphisms from UCE loci and COI sequences to analyze species boundaries based on nuclear and mitochondrial DNA. We recovered a monophyletic *Tapinoma* with an estimated crown age corresponding to middle Eocene (49.4 to 34.4 Ma). Phylogenomic data differentiated *T. melanocephalum* from *T. jandai*, a recently established species based on morphology, and revealed that the 2 species diverged ~12 Ma. Population genetic analyses identified considerable molecular divergence among sampled *T. melanocephalum* populations, and a heterogeneous genetic structure, showing a weak relationship between genetic differentiation and geographic distance. A phylogeographic comparison of habitat preferences of *T. melanocephalum* revealed an ecological shift from undisturbed to urban environments, a phenomenon which may have facilitated its ubiquitous and global distribution. Our study presents the first phylogenomic framework for this globally distributed ant genus and molecularly delineates a worldwide pest ant species.

Keywords: biogeography, tramp species, molecular systematics, Tapinomini, ultraconserved elements

Received: 8 November 2024. **Revised:** 13 June 2025. **Accepted:** 13 August 2025

Graphical abstract

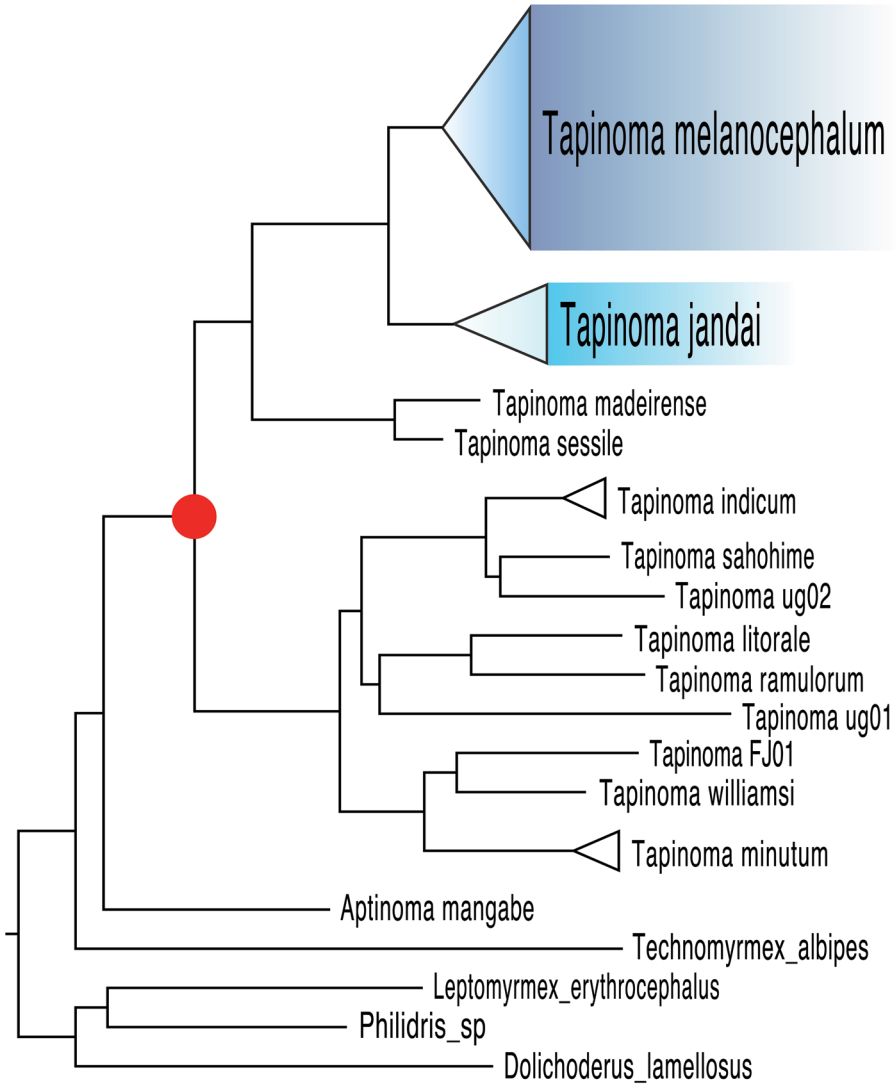

Introduction

Ants of the genus *Tapinoma* Foerster, 1850 (Dolichoderinae: Tapinomini) have a global distribution and broad ecological preferences. They inhabit diverse environments, from grasslands to rain forests, and use a wide variety of nest sites (eg in soil, under stones, in rotten wood, in dead stems, under epiphytes, and in carton nests under leaves—Wetterer 2009, LaPolla et al. 2010, Ward 2010). They are generalized foragers (Wheeler 1922, Bolton 1973, Brown 2000) with a preference for honeydew, and they often tend hemipterans (Bolton 1973, Shattuck 1992).

The genus *Tapinoma* was established by Foerster in 1850 and currently comprises 81 extant species plus an additional 24 valid subspecies and 6 fossil species (Bolton 2024). The present diversity of the genus does not seem to follow a strong latitudinal gradient, as many subtropical regions have reported higher species richness than many tropical countries. However, this pattern may be due to the lack of systematic studies and undersampling in many tropical areas (Janicki et al. 2016, Kass et al. 2022). Some lineages of *Tapinoma* are taxonomically challenging due to their perceived lack of morphologically distinct characters that can be used in identification (Seifert et al. 2024). Thus, it is likely that the species richness of the genus is still underestimated.

Ward et al. (2010) studied the phylogenetic relationships of the subfamily Dolichoderinae and recovered the tribe Tapinomini as sister to the remaining dolichoderines (Bothriomyrmecini + [Dolichoderini + Leptomyrmecini]). Divergence times estimated for the subfamily range between 67 and 96.6 Ma (Moreau et al. 2006, Ward et al. 2010, Moreau and Bell 2013). Within Tapinomini, *Tapinoma* was recovered as the sister group of *Aptinoma* (Ward et al. 2010). There are few taxonomic studies of *Tapinoma*, the studies that have been done have focused on individual species or regions (eg Seifert 2012, García-Avendaño and Guerrero 2018, Guerrero 2018,

Escárraga et al. 2021, Guerrero 2021, Seifert 2022, Seifert et al. 2024), and this limited scope underscores the need to address the broader lack of information for species identification, as well as the potential underestimation of species richness within the genus. Furthermore, to date, there is no comprehensive taxonomic revision of *Tapinoma* nor a species-level phylogenetic study of the genus.

Tapinoma melanocephalum (Fabricius 1793)

The most notorious member of the genus is the "ghost ant" *Tapinoma melanocephalum* (Fabricius 1793), which is one of the most broadly distributed species of ants on the planet. Although it is primarily a tropical and subtropical species, it has invaded temperate regions where it is usually restricted to indoor habitats (Wilson 1967, Espadaler and Espejo 2002, Guerrero 2018). It is an opportunistic nester and has become a ubiquitous nuisance pest in homes, greenhouses, or other buildings where warm temperatures prevail throughout the year. Although it is most common in disturbed habitats and human settlements (Shattuck 1992, Wetterer 2009, Guerrero 2018), it is also sometimes found in primary forests and other intact habitats and can be a member of local ant assemblages (Janda and Konecna 2011, Klimes et al. 2011).

The success of the species is attributed to its remarkable social structure and life strategy. The colonies contain numerous reproductive females (polygyny), and queens may be spread out in numerous subcolonies (polydomy) (Guerrero 2018). The new colonies are often formed by budding and mating is reported to be intranidal (Smith and Whitman 1992). These features allow the species to occupy temporary habitats and facilitate rapid and frequent migrations of the colonies (Appel et al. 2004, Wetterer 2009). A regional study of genetic structure of populations from South China revealed rather low relatedness among colonies, but also low mtDNA diversity within colonies, suggesting that polygyny is secondary, resulting from a single foundress (Zheng et al. 2018). Although parthenogenetic reproduction has been suggested, there is no direct evidence for it so far (Bustos and Cherix 1998). Although *T. melanocephalum* does not appear to cause strongly negative impacts on biomes it has invaded as other highly invasive ants such as *Linepithema humile* (Mayr 1868), *Wasmannia auropunctata* (Roger 1863), or *Tapinoma nigerrimum* (Nylander 1856) complex, it is still one of the most problematic urban pests on the planet. There are documented cases of its adverse effects on local biodiversity or agriculture, and it can be an important pathogen vector (Moreira et al. 2005). It is considered a major motivator for insecticide use in and around human habitations (Greenberg et al. 2010, Luo and Chang 2013). Negative impacts on agriculture are the result of symbiotic associations with Hemiptera, which cause damage to plants and promote the spread of diseases in agricultural systems (Venkataramaiah and Rehman 1989, Fowler et al. 1993).

The ghost ant is among the first ants with a documented global presence. Most of the earliest records are from the second half of the 19th century in Asia and Oceania, but the original description of the species comes from French Guyana in 1793 (Wetterer 2009). Surprisingly, the origin of the species is still uncertain and both Asia and the Neotropics have been proposed (Wetterer 2009, Janicki et al. 2016, Guerrero 2018). The current consensus, supported by its morphological resemblance to other Asian species (*T. indicum*, *T. minutum*, and *T. jandai*) and its common presence in disturbed areas and primary habitats in both regions, is that *T. melanocephalum* originated in Asia or the Indo-Pacific (Wetterer 2009). Wetterer (2009) also points out that many New World records might have been restricted initially to coastal areas and other regions often affected by global trade and invasive species. Some circumstantial evidence for the ghost ant being native to the South Asian region (Janicki et al. 2016) was provided by Seifert (2022), who used morphometric data to show that Asian material previously identified as *T. melanocephalum* actually comprised 2 cryptic species. The undescribed member of the pair was originally given the name *T. pithecorum* (Seifert 2022), but further comparison revealed that its type series was a rare color variant of *T. pygmaeum*, and thus, the species was recently redescribed as *T. jandai* (Seifert 2025).

This study aims to (1) establish the first phylogenetic framework for the genus *Tapinoma* based on genome-scale data and (2) examine the geographic origin, genetic diversity, and habitat preferences of the ubiquitous, tramp species *T. melanocephalum*. By including multiple specimens from throughout the range of this species, we explore phylogeographic patterns and assess molecular divergence between the recently described species *T. jandai* and populations of *T. melanocelphalum*, revealing the potential for additional cryptic species. Lastly, (3) we provide a hypothesis on divergence times and biogeographic history of the genus.

Materials and Methods

Taxon Selection

We obtained UCE sequence data for 28 specimens: 23 *Tapinoma* plus 5 additional outgroup specimens from the genera *Aptinoma* Fisher 2009, *Dolichoderus* Lund 1831, *Leptomyrmex* Mayr 1862, *Philidris* Shattuck 1992, and *Technomyrmex* Mayr 1872. The data for 24 specimens were newly generated for this study, and data for 4 specimens were taken from Branstetter et al. (2017) (BioSample number: SAMN06208935, SAMN06208899, SAMN06208912, and SAMN06208954). The specimens originated from diverse regional projects focusing on the ecology and systematics of ants and were either stored in 96% ethanol or dry-mounted before sequencing. Due to the genus's global distribution, we aimed to include representatives from all continents and major biogeographic regions. Australasian and Oriental samples comprise a larger portion of our dataset to better assess the potential origin of *T. melanocephalum* in these areas. In contrast, African samples are underrepresented due to limited availability of genomic material from the region. The localities and biogeographic region for samples are in Table 1, and detailed sample data are listed in Table S1.

UCE Sequencing

We examined phylogenetic relationships and species boundaries among *Tapinoma* species and populations following the UCE methodology described in Branstetter et al. (2017). These protocols include DNA extraction, sample quality control, DNA fragmentation (400–600 bp), library preparation, library pooling (equimolar pools of 10 samples), UCE enrichment, qPCR quantification, and final pooling (~100 total samples per sequencing pool), which were carried out at the University of Utah. To enrich the UCE loci, we used a customized ant bait set ("ant-specific hym-v2") that includes 9,898 baits (120 mer) targeting 2,524 UCE loci shared across Hymenoptera (Branstetter et al. 2017). The UCE sequencing was performed on an

Table 1. List of specimens used for UCE analysis

Sample ID	Collect Acc. No.	BioSample	Locality	Biogeographic region
Aptinoma_mangabe_EX1742	BLF31936	SAMN33554211	Madagascar	African
Dolichoderus_lamellosus_EX843 [a]	JTL8604	SAMN06208899	Costa Rica	African
Leptomyrmex_erythrocephalus_EX1644 [a]	PSW13808	SAMN06208912	Australia	Neotropical
Philidris_sp_EX1581 [a]	JTL8846-s	SAMN06208935	Malaysia	Australasian
Tapinoma_FJ01_EX1748	FBA519633	SAMN33554212	Fiji	Australasian
Tapinoma_indicum_cf_EX1734	HP0049	SAMN33554213	Papua New Guinea	Australasia/Oriental
Tapinoma_indicum_EX1747	EPE255	SAMN33554214	Fiji	Australasian/Oriental
Tapinoma_litorale_EX1752	JTL9633	SAMN33554215	Mexico-Oaxaca	Neotropical/Nearctic
Tapinoma_madeirense_EX1736	MLB54	SAMN33554216	Poland	Palaearctic
Tapinoma_melanocephalum_MJ30955	B6-NAG-I-II/0138	SAMN33554217	Papua New Guinea	Australasian/All
Tapinoma_melanocephalum_EX1731	MJ13372	SAMN33554218	Papua New Guinea	Australasian/All
Tapinoma_melanocephalum_EX1732	JCM0115A	SAMN33554219	Palau-Koror	Oriental/All
Tapinoma_melanocephalum_EX1737	GUA0498	SAMN33554220	Salomon-Guadalcanal	Australasian/All
Tapinoma_melanocephalum_EX1738	RJGF-030	SAMN33554221	Colombia-Santander	Neotropical/All
Tapinoma_melanocephalum_EX1743	EMS2469.02	SAMN33554222	Fiji	Australasian/All
Tapinoma_melanocephalum_EX1744	OK00380	SAMN33554223	Japan	Oriental/All
Tapinoma_minutum_EX1729	PF165	SAMN33554224	French Polynesia	Australasian
Tapinoma_minutum_MJ21395	MJ21395	SAMN33554225	Australia	Australasian
Tapinoma_jandai_cf_EX1730	MJ13328	SAMN33554226	Palau-Koror	Oriental
Tapinoma_jandai_EX1745	BDB024	SAMN33554227	China	Oriental
Tapinoma_jandai_EX1750	Bharti20160512	SAMN33554228	India	Oriental
Tapinoma_ramulorum_EX1751	JTL9041	SAMN33554229	Panama	Neotropical
Tapinoma_sahohime_EX1746	OK00855	SAMN33554230	Japan	Oriental
Tapinoma_sessile_EX1584 [a]	JTL8166	SAMN06208954	United States	Nearctic
Tapinoma_UG01_EX1740	BLF29708	SAMN33554231	Uganda	African
Tapinoma_UG02_EX1741	BLF29528	SAMN33554232	Uganda	African
Tapinoma_williamsi_aff_EX1733	HP0038	SAMN33554233	Papua New Guinea	Australasian/Oriental
Technomyrmex_albipes_BBX548	BLF17989	SAMN33554234	Madagascar	African/Oriental

For *T. melanocephalum*, a globally widespread species, only the regions of the collecting site are listed. The detailed locality data are in Table S1.
[a]Samples from Branstetter et al. (2017).

Illumina HiSeq 2500 instrument (2 × 125 bp v4 chemistry; Illumina Inc., San Diego, CA) at the University of Utah (High-Throughput Genomics Core Facility). The raw sequences have further been submitted to NCBI (BioProject PRJNA939201) (Table S1). All datasets for phylogenetic and posterior analyses are available in the Figshare data repository (https://figshare.com/s/34b49e0034d672819f18).

UCE Matrix Generation

The sequence data were cleaned using Phyluce 1.7.1 (Faircloth 2016) and de-novo assembled with SPAdes 3.13.0 (Nurk et al. 2017). Within the Phyluce environment, we used the programs Illumiprocessor 2.0 (Faircloth 2013), which incorporates Trimmomatic (Bolger et al. 2014), for quality trimming raw reads, and LASTZ 1.0 (Harris 2007) for identifying the targeted UCE loci from all de-novo assembled contigs based on the ant-specific hym-v2 bait sequences file. To calculate assembly statistics, including sequencing coverage, we used scripts from the Phyluce package (phyluce_assembly_get_spades_coverage and phyluce_assembly_get_spades_coverage_for_uce_loci), which use the programs BWA 0.7.7 (Li and Durbin 2010) and GATK 3.4.0 (McKenna et al. 2010).

After extracting UCE contigs, we aligned each UCE locus using a standalone version of the program MAFFT 7.130 b (Katoh and Standley 2013) and the L-INS-i algorithm. We then used a Phyluce script to trim flanking regions and poorly aligned internal regions using the program Gblocks (Talavera and Castresana 2007). The program was run with reduced stringency parameters (b1:0.5, b2:0.5, b3:12, and b4:7). We then used another Phyluce script to filter the initial set of alignments so that each alignment was required to include data for ≥75% of taxa. To calculate summary statistics for the final data matrix, we used a script from the PHYLUCE package (phyluce_align_get_align_summary_data). All steps, including the phylogenetic analyses described below, were performed on a multicore hybrid cluster (2880 GPUs cores) in the Laboratorio Nacional de Análisis y Síntesis Ecológica LANASE, UNAM and on the MetaCentrum cluster in the Czech Republic.

Phylogenomic Analysis

We inferred phylogenetic relationships of *Tapinoma* species with the likelihood-based program IQ-TREE 2.2.2.6 (Minh et al. 2020). To partition the UCE data for phylogenetic analysis, we used the sliding-window site characteristics based on entropy (SWSC-EN) algorithm (Tagliacollo and Lanfear 2018). The resulting data subsets were merged using PartitionFinder 2.1.1 (Lanfear et al. 2012, Lanfear et al. 2017), with the rclusterf algorithm, AICc model selection criterion, and the GTR+G model of sequence evolution. For the IQ-TREE analysis, we used the partition scheme suggested by PartitionFinder 2 and the jModelTest/ModelFinder (-m TEST/MF) to select the best substitution models under the Akaike Information Criterion (AIC). To assess branch support, we performed 1,000 replicates of the ultrafast bootstrap approximation (UFB) (Minh et al. 2013, Hoang et al. 2018), and 1,000 replicates of the branch-based, Shimodaira–Hasegawa approximate likelihood ratio

test (Guindon et al. 2010). To obtain an alternative assessment of relationships and branch supports, we conducted a coalescent-based species tree analysis on the dataset using the summary program ASTRAL-III 5.7.4 (Zhang et al. 2017). First, we estimated gene trees per locus in the program IQ-TREE under the GTR+G model. Second, a standard ASTRAL analysis was conducted with the gene trees as input, leaving all terminals as separate entities and assessing support as local posterior probabilities. The species tree and gene trees were used to calculate the gene concordance factor (gCF) and the site concordance factor (sCF) in IQ-TREE.

Divergence Dating

Divergence dates within *Tapinoma* were inferred in IQ-TREE with the same dataset, partitions, and models as the phylogenetic analysis. The tree topology was constrained to the relationships recovered by the maximum likelihood analysis. We ran the Least Square Dating (LSD) method, applying a uniform distribution model, with relaxed clock. Three calibration points were assigned with uncertainty intervals, based on previous studies (Moreau et al. 2006, Perkovsky et al. 2007, Moreau and Bell 2013, Barden 2017): *Dolichoderus* + (*Leptomyrmex* + *Philidris*) (min=-67: max=-53.5: as stem age of outgroups); *Tapinoma* (min=-53: max=-40.5: as a conservative stem age); and the fossil *T. troche* Wilson, 1985 from Miocene Dominican amber (min=-20: max=-16) for *T. litorale* clade (R. Guerrero, personal communication). The root was constrained to -79, representing the oldest known age for the subfamily based on fossil evidence (Dlussky 1999, Barden 2017).

For an alternative divergence-dating analysis, we used BEAST 2.6.3 (Drummond et al. 2012, Bouckaert et al. 2019) and restricted this analysis to a subset of UCE loci, due to computational constraints. Using the script gene_stats (Borowiec et al. 2015), we calculated the average bootstrap support for each locus in R (R Core Team 2020) and used the results to create a dataset consisting only of the 100 UCE loci with the highest bootstrap support from our 100% complete dataset. We used the same calibration points as in the LSD analysis. For the secondary calibration priors we selected log-normal distributions, means in real space and assigned: *Dolichoderus* prior (stem age) M = 60.0 and S = 0.07, *Tapinoma* prior (stem age) M = 46.0 and S = 0.085. We selected a log-normal distribution for the fossil *T. troche* prior and assigned M = 18.0 and S = 0.07. For the analysis, we used a GTR+G model of sequence evolution with 4 gamma rate categories, an uncorrelated log-normal clock, and a birth–death tree prior. We performed 4 independent runs, each for 500 M generations, sampling a single tree every 50 K. Runs were combined and summarized using LogCombiner. A Maximum Clade Credibility tree (MCC) was generated in TreeAnnotator after eliminating the first 5,000 trees as burn-in. Convergence of the MCMC and effective sample sizes (ESS) above 200 were checked in Tracer 1.7.1 (Rambaut et al. 2018).

Biogeographic Analysis

To infer ancestral areas, we used the multimodel BioGeoBEARS approach (Matzke 2012, 2013) implemented in R (R Core Team 2020) with the MCC chronogram from the BEAST 2 analysis as input. We pruned all outgroup taxa from the tree except for *Technomyrmex albipes* and *Aptinoma mangabe*. We constructed a species distribution matrix based on biogeographic regions where representatives of the clades are distributed, and denoted as AF = African, AU = Australasian, NA = Nearctic, NE = Neotropical, OR = Oriental, and PA = Palaearctic. We assigned all known distributions for the terminal taxa and all biogeographic regions for *T. melanocephalum*. We ran the program with 6 models (DEC, DIVALIKE, and BAYAREALIKE and each with the jump dispersal parameter J), setting the maximum ancestral species range to 6 units, with no dispersal limitation between areas, and compared model results via LnL, AIC, and AICc scores.

Calling SNPs from UCEs for *Tapinoma* Delimitation Analysis

To compare genetic differences in lineages of *T. melanocephalum*, single nucleotide polymorphisms (SNPS) were extracted from UCE loci. We built 2 different datasets, one with all UCE sequences of *Tapinoma* species (22) and the other only with *T. melanocephalum* and *T. jandai* specimens (10) (*T. melanocephalum* + *T. jandai* matrix). In these sets, the individual with the largest number of UCE contigs as identified by phyluce_assembly_get_match_counts was chosen as a reference individual for SNP calling. The programs phyluce_assembly_get_match_counts and phyluce_assembly_get_fastas_from_match_count were re-run on the reference individual to create a fasta of UCE and exon contigs found just in the reference. Reference loci were indexed using BWA 0.7.17 (Li and Durbin 2010). BAM files for each individual in the analysis were created by mapping their reads to the reference using BWA-MEM (Li 2013), sorting the reads using SAMtools 1.11 (Li et al. 2009) and removing duplicates using Picard 2.24.0 (http://broadinstitute.github.io/picard/). GATK was then used to realign BAMs around indels, call variants, and filter variants based on VCFtools 0.1.13 (Danecek et al. 2011). For each clade, biallelic SNPs were called at loci for which at least 75% of taxa were represented and for which at least 10 reads were mapped to each locus. SNPs were filtered to one SNP per locus for loci < 1,000 bp.

After thinning, the VCF file was reformatted to STRUCTURE and NEXUS formats using PGDSpider 2.1.0.3 (Lischer and Excoffier 2012). We used STRUCTURE 2.3.4 (Pritchard et al. 2000) to explore the limits of genetic structure between *T. melanocephalum* and *T. jandai* with a Bayesian clustering approach. The analysis was performed using an admixture model and 1M generations with 250 K generations as burn-in and 5 replicates for each K (K = 10) which led to convergence for all analyses. Clusters of species and populations assumptions (K) were estimated with a Discriminant Analysis of Principal Components (DAPC) (Jombart et al. 2010), using the adegenet package 2.1.3 (Jombart 2008) in R (R Core Team 2020), and tested different K values (K = 2, 3, 5, 10).

We generated a coalescent-based species tree from the SNPs data using SNAPP 1.5.1 (Bryant et al. 2012). For this analysis, we started with no a priori assumptions about how individuals grouped into clusters to allow the program to inform the number of lineages to visualize potential genetic connections among individuals in DensiTree 2.6.3 (Bouckaert 2010, Bouckaert and Heled 2014). Posteriorly, we ran an additional 4 sets of *T. melanocephalum* and *T. jandai* (Table 3) to compare species delimitation models and calculated their bayes factors. We ran the SNAPP analysis using BEAST 2 using default settings and 50M generations, sampling log and tree frequencies every 50K.

COI Matrix Generation

All cytochrome c oxidase (COI) sequences of *Tapinoma* species currently available from public databases were used for an additional species delimitation and phylogeographic analysis. For this analysis, we extracted COI sequences from our UCE-enriched samples, using a complete barcode sequence of *T. melanocephalum* from BOLD (Acc.# ASAMZ253-07) as a bait input sequence for a Phyluce script (phyluce_assembly_match_contigs_to_barcodes) that extracts COI sequences from bulk sets of contigs. We expanded this dataset by sequencing additional COI sequences from 81 samples representing diverse world populations of *T. melanocephalum*. Finally, we included 66 accessible *Tapinoma* species barcode sequences from BOLD (Ratnasingham and Hebert 2007) and 49 from GenBank. After cleaning the matrix to avoid repeated sequences, the combined dataset (Table S2) was aligned using MAFFT, and visually inspected in Mesquite 3.2 (Maddison and Maddison 2018). To minimize the use of misidentified specimens, which may occur in BOLD and GenBank, we included only sequences that had a minimal length overlap of 75%, that were congruent and had >90% similarity with lineages of the identified species, and that did not cause species to be polyphyletic in preliminary analyses. We also did not consider any sequence with stop codons to avoid use of pseudogenes and NUMTS. The complete aligned matrix included 217 COI sequences of 21 tentative species, 138 of them assigned to *T. melanocephalum*.

Two matrices were built: (i) *Tapinoma* matrix with 107 sequences from 21 tentative species and with 47 selected sequences of *T. melanocephalum* to avoid over-parameterization of the populations; and (ii) *T. melanocephalum* matrix with 138 sequences from different populations of this species.

Tapinoma COI Species Delimitation Analysis

Three approaches were used to delimit *Tapinoma* species: Bayesian Poisson Tree Processes (bPTP) (Zhang et al. 2013, Kapli et al. 2017), Multi-rate Poisson Tree Processes (mPTP) (Kapli et al. 2017), and General Mixed Yule Coalescent (GMYC) (Pons et al. 2006) with the *Tapinoma* matrix which included 108 COI sequences. This matrix was partitioned by codon position and analyzed with IQ-TREE using the best model selection under ModelTest with the "–m MFP" option, 1,000 ultrafast bootstrap replicates, and 1,000 SH-like replicates. The bPTP analysis was run on the IQ-TREE gene tree with default options: rooted tree, MCMC generations = 100 000, Thinning = 100, Burn-in = 0.1, Seed = 123 in the bPTP web server (https://species.h-its.org/). The mPTP analysis was carried out with default parameters in the mPTP web server (https://mptp.h-its.org/). For GMYC analysis, a preliminary Bayesian tree was constructed in BEAST 2, under a lognormal relaxed clock, coalescent constant population prior and 50M generations, sampling log and tree frequencies every 50K. Finally, we used the ultrametric tree to delimit species with the SPLITS package (Ezard et al. 2009) implemented in R ("splits","repos="; http://R-Forge.R-project.org), under a single threshold optimization.

Tapinoma melanocephalum Population Genetic Analyses

We used the COI matrix containing *T. melanocephalum* (138 sequences) and *T. jandai* (19 sequences) to evaluate genetic variation, population structure, and Analysis of Molecular Variance (AMOVA) in Arlequin 3.5.2 (Excoffier and Lischer 2010) and GenAlEx 6.51b2 (Peakall and Smouse 2012). The COI sequences were structured by localities (populations) and biogeographic regions (groups) for comparison ($n \geq 6$), independently for each species (Table S2). We calculated gene flow, genetic differentiation, descriptive statistics (h, hd, π, S), neutrality tests (Tajima's D, Fu's Fs, R_2), and the number of haplotypes in DNAsp 6 (Rozas et al. 2017), and generated a haplotype network, with the Median-joining network option in PopART (Leigh and Bryant 2015). Additionally, we constructed a haplotype tree in IQ-TREE using the best model selection under jModelTest with the "–m TEST" option, 1,000 ultrafast bootstrap replicates, and 1,000 SH-like replicates. We conducted a Principal Component Analysis (PCA) on the COI sequence data using adegenet (Jombart 2008) and ade4 (Dray and Dufour 2007) to confirm our *Tapinoma* population identifications. Finally, we ran an isolation-by-distance test (IBD) (Diniz-Filho et al. 2013) only for *T. melanocephalum* sequences.

Habitat Preference Reconstruction

We examined the evolution of habitat preferences of *T. melanocephalum* and *T. jandai* populations using ancestral state reconstruction, taking into account collection sites and data using the program BayesTraits 3.0.2 (Pagel and Meade 2017). We used 3 states in the habitat preference reconstruction: 0 = natural or undisturbed zone (primary or secondary vegetation), 1 = disturbed zone (transition between natural and urban), and 2 = urban zone (highly disturbed synanthropic habitats). This analysis was performed on all 1001 trees obtained from preliminary BEAST 2 analysis and the trait–habitat combinations. We ran BayesTraits using Montecarlo Markov Chain (MCMC) method, multistate trait-habitat, 100 K iterations, and 10% burn-in. All analyses in BayesTraits were repeated 3 times to check the congruence of independent runs.

Results

UCE Alignment

The assembly of cleaned reads produced an average of 133,353 contigs per sample (range: 70,160-216,853 contigs). After sequencing, assembly, and extracting contigs representing UCE loci from 28 specimens, we recovered an average per contig coverage of 38.4× (range: 16.4–56.4×) and a mean contig length of 665.34 bp (range: 305–1,835 bp). Following alignment, trimming, and filtering of the UCE contigs, our UCE matrix (≥75% of taxa) consisted of 2,271 loci and 1,583,275 bp of sequence data, of which 316,855 bp were informative. The mean alignment length post-trimming was 697.17 bp (range: 191 to 1,428 bp). The final matrix included only 12.7% of missing data (including gaps). The results of the best-fit partitioning scheme from PartitionFinder included 1,676 subsets and had a significantly better log-likelihood than alternative partitioning schemes.

Phylogeny and Divergence Time Estimations

The genus *Tapinoma* was recovered as monophyletic with *Aptinoma* as its sister group. Within *Tapinoma*, 2 main clades were recovered. The first clade (with *T. indicum*) contains several Old World species, including 2 separate African lineages and 2 separate Australasian-Oriental lineages. Embedded within them is a Neotropical-Nearctic diversification. The second clade

contains Oriental and Australasian *T. melanocephalum*, its cryptic sister species *T. jandai*, and a clade of Palaearctic and Nearctic species (*T. sessile* and *T. madeirense*). The UCE phylogenies recovered in IQ-TREE and ASTRAL (Fig. 1) showed the same robust hypothesis for *Tapinoma* species relationships with most nodes receiving maximum bootstrap (100) and approximate likelihood ratio test (100) support. The concordance factors (gCF and sCF ≥ 85) also strongly supported the resulting topology.

The estimated divergence times in BEAST (Fig. 2) suggest a crown-group origin of the genus in the Middle Eocene, 41.6 Ma (95% HPD 49.4:34.4 Ma), in line with the estimates under the Least Square Dating method in IQ-TREE. Divergence time estimation under the Least Square Dating method (Fig. S1) suggested an origin of the genus *Tapinoma* 47.13 Ma. The estimated origin for the crown group ranged between 37 and 11 Ma (95% HPD), between the Oligocene and Middle Miocene. We estimated the divergence event between *T. melanocephalum* and *T. jandai* in the Lower Miocene and Upper Miocene, 13.1 Ma (95% HPD 20.8: 6.4 Ma). The origin for *T. melanocephalum* was estimated to be Pliocene or Pleistocene (95% HPD 5.1: 1.2 Ma).

Biogeographic Reconstruction

The BioGeoBEARS analysis suggested that including the founder-event speciation (+J) in DEC, DIVALIKE, and BAYAREALIKE models significantly improved the likelihood. The DEC+J model (Table 2; Fig. S2) had the best scores compared to the alternative models (-LnL = -78.9, AIC = 153.8, and AICc = 154.7).

The ancestral area for the genus *Tapinoma* appears to be within the Australasian biogeographic region (recovering a lower probability for the Oriental region and Australasian + Oriental), with a subsequent dispersal to other regions. The first reconstructed event occurred between ~40 and 20 Ma in the lineage that divided species with Nearctic—Palaearctic distribution (*T. sessile*, *T. madeirense*) and (*T. melanocephalum* + *T. jandai*) from the remaining species. Another dispersal event

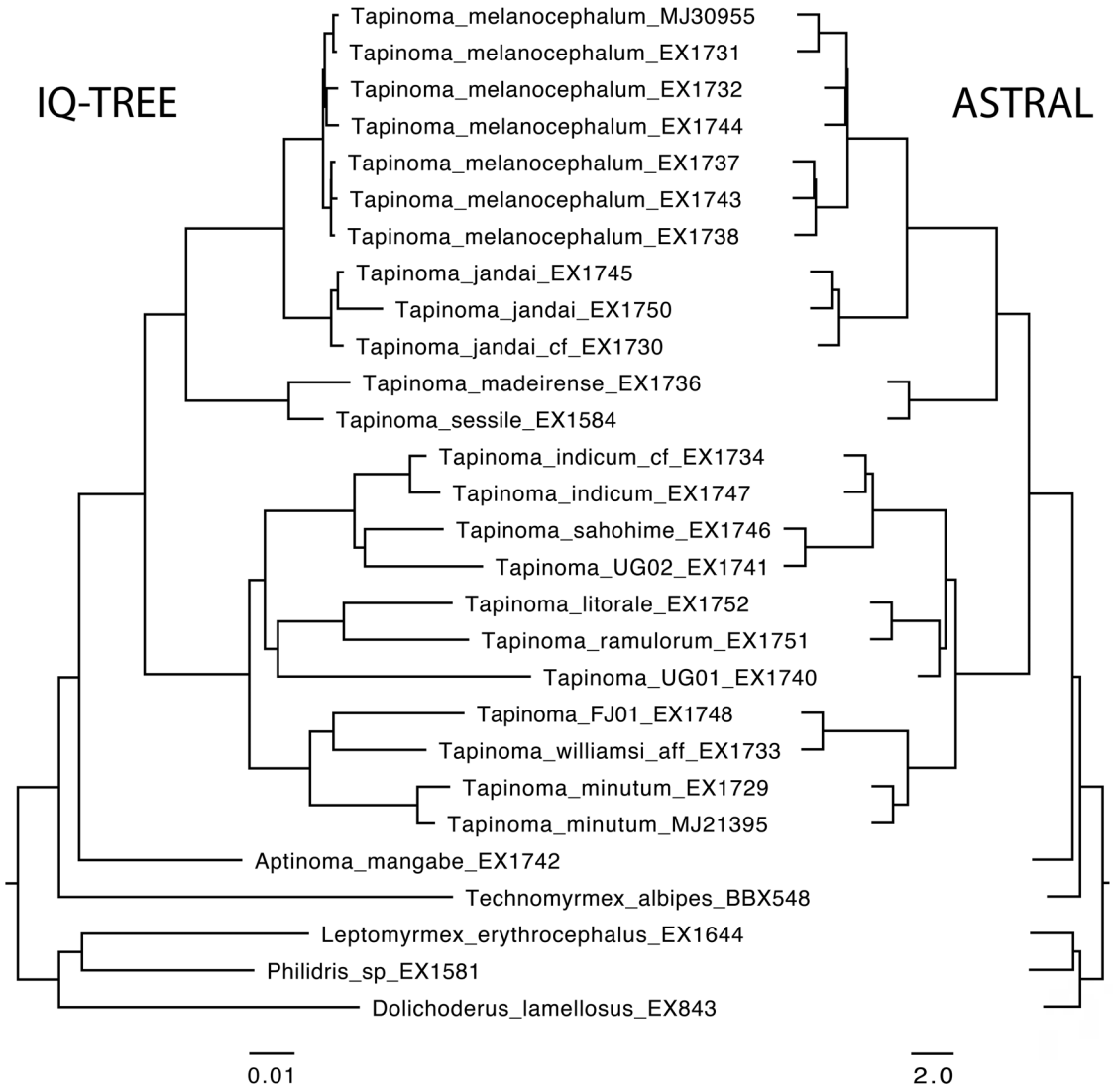

Fig. 1. Phylogeny of *Tapinoma*. Topology on the left is inferred using the program IQ-TREE and 2,271 UCE loci. Node support is only labelled in nodes with less than maximum support (values = ultrafast bootstrap/SH-like). Terminal names show sample ID. Topology on the right represents species tree estimated using the program ASTRAL III from 2,271 UCE gene trees. All nodes have a maximum node support = local posterior probabilities (LPP).

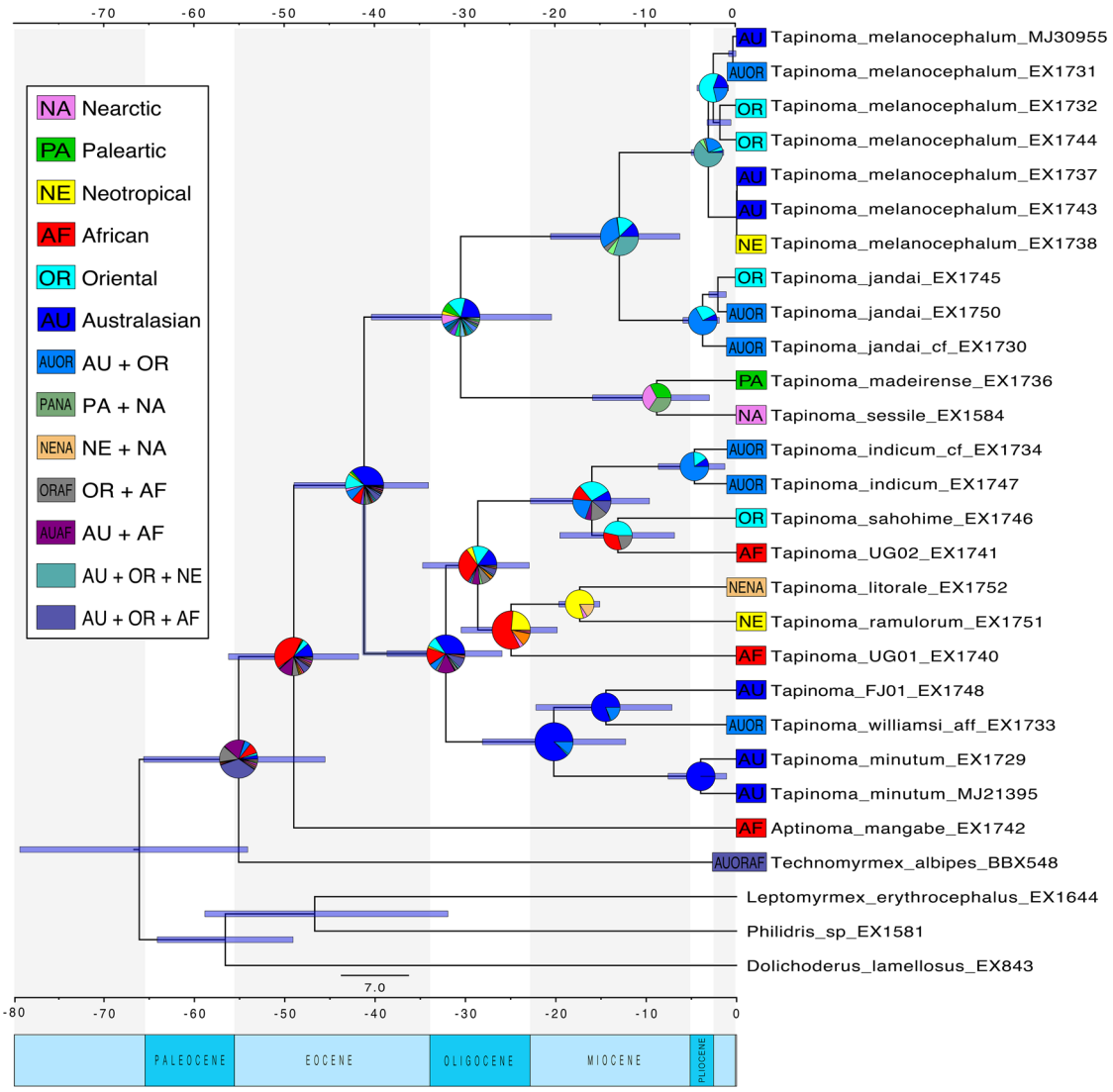

Fig. 2. Ultrametric tree of *Tapinoma* recovered in BEAST and BioGeoBEARS (DEC+J) using 100 BEST UCE loci. Bars on nodes depict 95% HPD (high posterior density) values. Pie charts on nodes indicate the most likely distribution areas of the most recent common ancestor (MRCA).

Table 2. Statistical values of the BioGeoBEARS analysis

Model	LnL	Params	d	E	j	AIC	AICc
DEC	-80.73	2	0.010	0.0091	0	155.5	0.0022
DEC+J	**-78.9**	**3**	**0.0014**	**1.0e-12**	**0.018**	**153.8**	**0.0020**
DIVALIKE	-92.66	2	0.011	0.0042	0	189.3	1.4e-08
DIVALIKE+J	-90.59	3	0.0081	1.0e-12	0.040	187.2	4.2e-08
BAYAREALIKE	-86.19	2	0.0065	0.034	0	156.4	0.20
BAYAREALIKE+J	-83.83	3	0.0017	0.015	0.029	154.7	0.79

The best fit model is bolded and based upon the LnL and AIC and AICc values.

separated the Oriental and Australasian lineages of *T. minutum*, *T. williamsi*, and *Tapinoma* FJ01 from the clade (*T. indicum* + [*T. sahohime* + *Tapinoma* UG01]) + (*Tapinoma* UG01 + [*T. Litorale* + *T. ramolorum*]). The next documented dispersal event divided these 2 groups between ~35 and 23 Ma, with an ancestral area in Africa (32.4%) or Australasian + Oriental (30.5%) regions for the most recent common ancestor (MRCA). One lineage included the species with Nearctic and Neotropical distribution (*T. litorale*, *T. ramolorum*) and *Tapinoma* UG01 from Africa. For the last group that included the species with Australasian and Oriental distribution (*T. sahohime*, *T. indicum*) and African *Tapinoma* UG02 (*T. cf subtile*), the ancestral area was recovered in the Oriental region. In the case of *T. melanocephalum* and *T. jandai*, the most probable ancestry in the Australasia + Oriental was followed by the expansion to other biogeographic regions. Although there were some slight

differences in the reconstruction of the ancestral areas on a few internal nodes (Table 2), both the DIVALIKE+J and the BAYAREALIKE+J models infer an ancestral Australasian or Oriental distribution for MRCA of *Tapinoma*.

SNP Analysis and Population Structure

The final matrix for *Tapinoma* contained 2,355 filtered SNPs, extracted from Gblocks cleaned alignments (2,545 UCE loci), while for *T. melanocephalum*, the matrix included 2,336 SNPs. The DAPC of the *Tapinoma* matrix suggested K = 12 and *T. melanocephalum* + *T. jandai* matrix indicated K = 2, matching the principal phylogenetic lineages. Both STRUCTURE and SNAPP analyses based on SNPs produced phylogenetic relationships that were congruent with the supermatrix results, including the separation of *T. melanocephalum* and *T. jandai*. However, the analysis revealed some mixing between several species (*T. sahohime* with *Tapinoma* UG02, *T. litorale* with *T. ramulorum*, and *T. williamsi* with *T. minutum*) (Fig. 3), which is also similar to the phylogenetic relationships of these species. For the *T. melanocephalum* + *T. jandai* matrix, STRUCTURE K = 2 revealed 2 independent clusters, while K = 3 and K = 5 showed a very low admixture between these 2 clusters, and K = 10 recovered the same clusters/groups as K = 2 (Fig. 3). For the SNAPP tree models tested, the best was the one that separated *T. jandai* (EX1730, EX1750, EX1745) and *T. melanocephalum* (Table 3, Fig. 3), which was also consistent with the genetic clusters in the STRUCTURE analysis (Fig. 3) and Nei's genetic distance (Fig. S3).

COI Tree and Species Delimitation

The final aligned matrix included 108 COI sequences of 21 species and was 654 bp in length. The COI sequences extracted from UCE data clustered well with conspecific sequences obtained by Sanger sequencing. We recovered the same groups of *Tapinoma* as in the UCE tree (Fig. 1), but with some different relationships among them, as the 2 datasets had different species selection (Fig. 4). Specifically, *T. williamsi*, *T. minutum*, and *T.* FJ01 were consistently members of the same clade, while the closely related *T. sessile* and *T. madeirense* formed another clade in both datasets. *T. jandai* was recovered as sister to *T. melanocephalum* and several of their sequences showed clustering by biogeographical region similar to the UCE tree (Fig. 2). The bPTP analysis recovered 23 MOTUs (molecular operational taxonomic units) with most nodes well-supported

Table 3. Model names of the alternative *T. melanocephalum* and *T. jandai* hypothesis

Model	# species	MLE	ln BF
All samples	1	-513.14	39.56
Oriental distributed/all other	2	-563.32	-3.37
T. jandai/*T. melanocephalum*	**2**	**-442.17**	**45.29**
Australasian/all other	2	-526.87	22.93
Neotropical/Oriental/Australasian	3	-587.92	-8.01

The best fit model is bolded. MLE, Marginal likelihood estimate; BF, Bayes Factor.

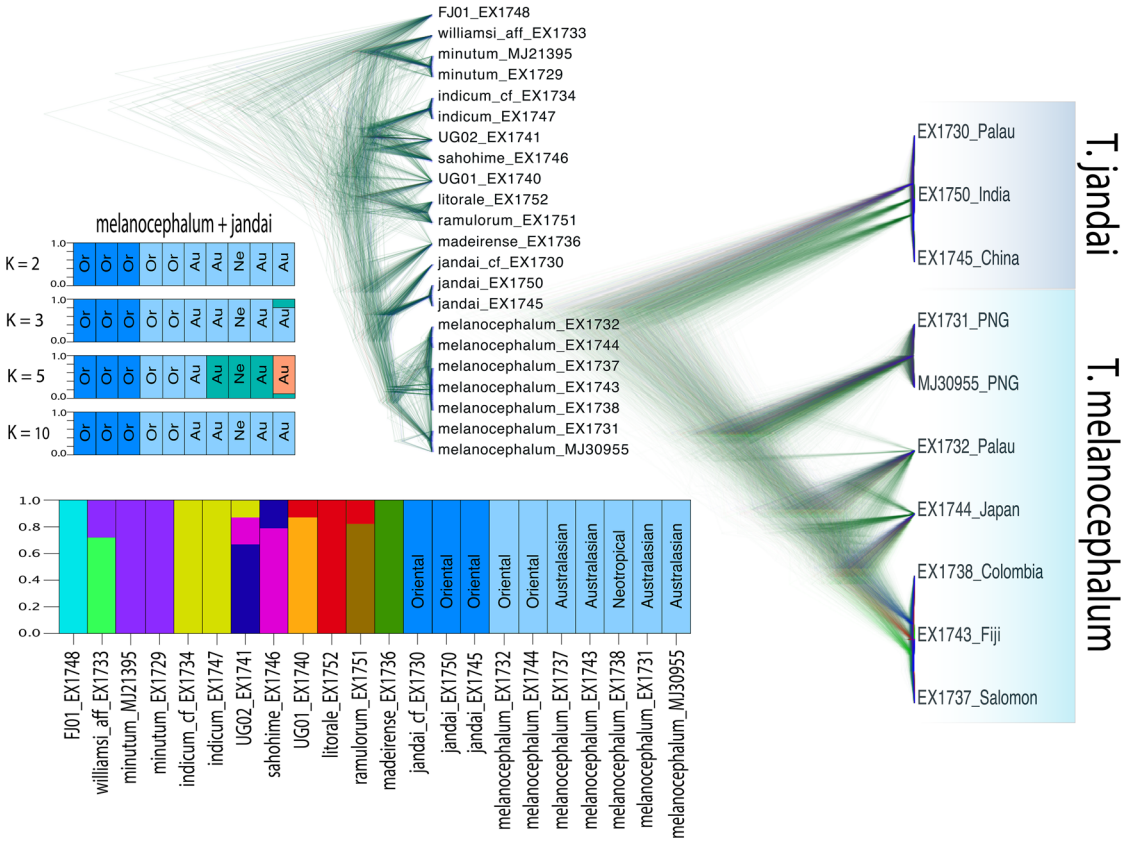

Fig. 3. Species tree cladograms for *Tapinoma* species (left, 2,408 SNPs) and for the *Tapinoma melanocephalum* clade (right, 2,336 SNPs) filtered from UCE loci. The bottom figure shows the probability of membership graph from STRUCTURE analysis. Terminal names show ID code and the locality of the samples.

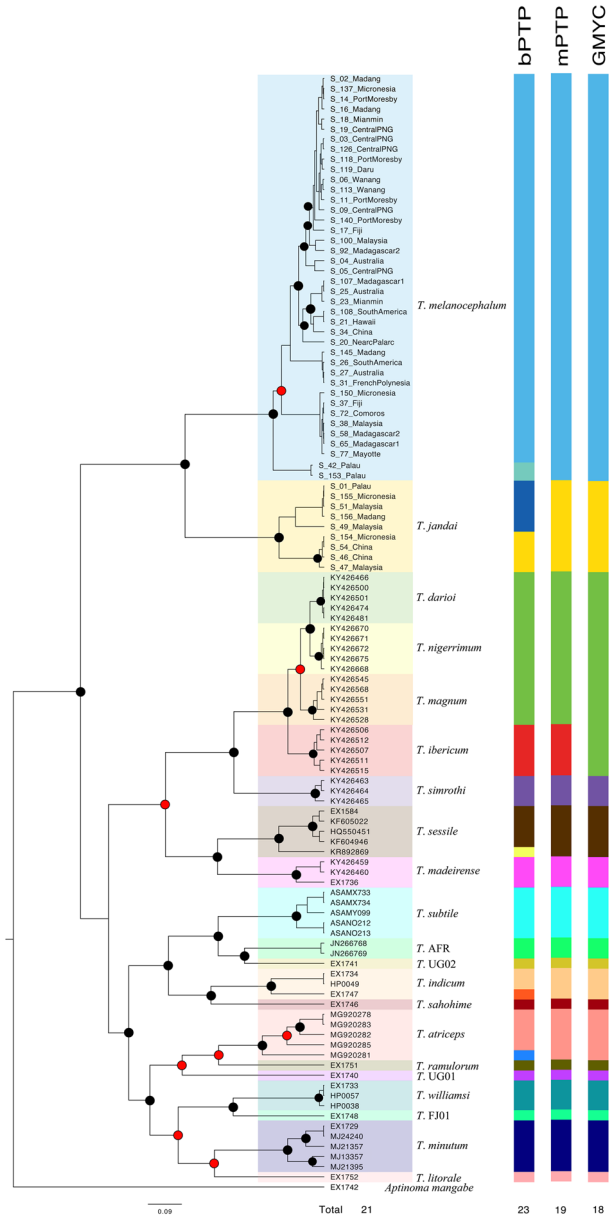

Fig. 4. Ultrametric tree inferred with BEAST, using a complete dataset for *Tapinoma* COI sequences. Circles on nodes denoted Posterior Probability, red circles = 0.80–0.90, black circles ≥ 0.90. Colored bars on the tree are original identifications of the vouchers based on morphology. Colors of bars on the right indicate different species delimited by bPTP, mPTP, and GMYC. The numbers below bars represent species recovered for each method.

(PP > 90), out of 21 *Tapinoma* species considered a priori by traditional taxonomy. The mPTP analysis recovered 19 MOTUs, with the best score for multi coalescent rate = 329.168 and null-model score = 329.168. While GMYC analysis recovered 18 MOTUs, with a confidence interval of 11-28, likelihood of null model = 591.224, and likelihood of GMYC model = 606.171. All 3 analyses were consistent in delimiting *T. melanocephalum* and *T. jandai* into 2 MOTUs. An inconsistency in this analysis occurred in the *T. nigerrimum* complex, where it was recovered as 1 (GMYC) or 2 (bPTP and mPTP) MOTUs. Although the species in this complex form 4 separate clades in our analysis, the phylogenetic distances (≤ 0.10) and calculated divergence times are low. A comprehensive analysis by Seifert et al. (2024) using microsatellite markers and morphological traits supports the existence of 4 species consistent with our 4 clades and 1 additional species not sampled here.

COI Population Genetic Analyses of the *T. melanocephalum* Clade

Ten COI mtDNA sequences for the *T. melanocephalum* clade were successfully extracted from UCE samples, 7 *T. melanocephalum* and 3 *T. jandai*. All our sequences of the COI fragment from 10 UCE samples and 81 separately sequenced samples had 654 bp in length. A total of 66 downloaded sequences from the Barcode of Life Database (BOLD), had lengths from 548 to 654 bp. This yielded a total of 138 COI sequences of *T. melanocephalum* for population analysis (Fig. 5). We obtained 63 haplotypes (h = 63) with 189 segregating sites, with a high haplotype diversity (Hd = 0.947) and a low nucleotide diversity (π = 0.069). We recovered 19 specimens of *T. jandai*, which were from the Oriental, Melanesian, and Micronesian regions. Table 4 shows the information by population. Neutrality tests Fu's F, Tajima's D, and Ramos-Onsins and Rozas (R_2) recovered significant values in most populations ($P < 0.02$). The haplotype network (Fig. 6) and principal component analysis (PCA) (Fig. S5) clustered most haplotypes by biogeographic region.

The AMOVA of *T. melanocephalum* showed greater variation among populations than within populations (Table 5). The variation between biogeographic regions is lower than among populations within regions. The isolation-by-distance analysis revealed a positive but not a strong correlation between genetic differentiation and geographic distance (r = 0.298, $P = 0.006$) (Fig. S6). The pattern of genetic differentiation value (mean Fst = 0.654) indicates a tendency for genetic structuring of populations mainly by biogeographic region. The Oriental *T. melanocephalum* populations differ from the rest, with the highest Fst values: ~1 (Fig. S4).

Evolution of Habitat Preferences

The habitat preference transition seems to be unidirectional from undisturbed and disturbed habitats to urban zones within *T. melanocephalum* and *T. jandai* (average of the values: q 0 2 = 1.638, q 1 2 = 1.672), with the most probable ancestral state in native undisturbed (mean: P 0 = 0.435) and disturbed habitat (mean: P 1 = 0.353). Shifts to urban habitats were recovered in multiple independent transitions. Although the overall pattern seems mixed, some internal clades represented groups from the same habitat (Fig. 5 and Fig. S7). The MRCA for populations of *T. melanocephalum* was a small Oriental lineage found in an undisturbed habitat. In *T. jandai*, the habitat switching pattern is similar: from undisturbed and disturbed areas to the urban habitat (MRCA mean: P 0 = 0.354, P 1 = 0.396) (Fig. S7).

Discussion

Phylogenetic and Biogeographic History of the Genus *Tapinoma*

The worldwide genus *Tapinoma* has been a taxonomically challenging group. We used UCE phylogenomic data and mitochondrial DNA to propose hypotheses about its phylogeny, divergence times, and general biogeographic history. We analyzed species boundaries of the globally widespread species

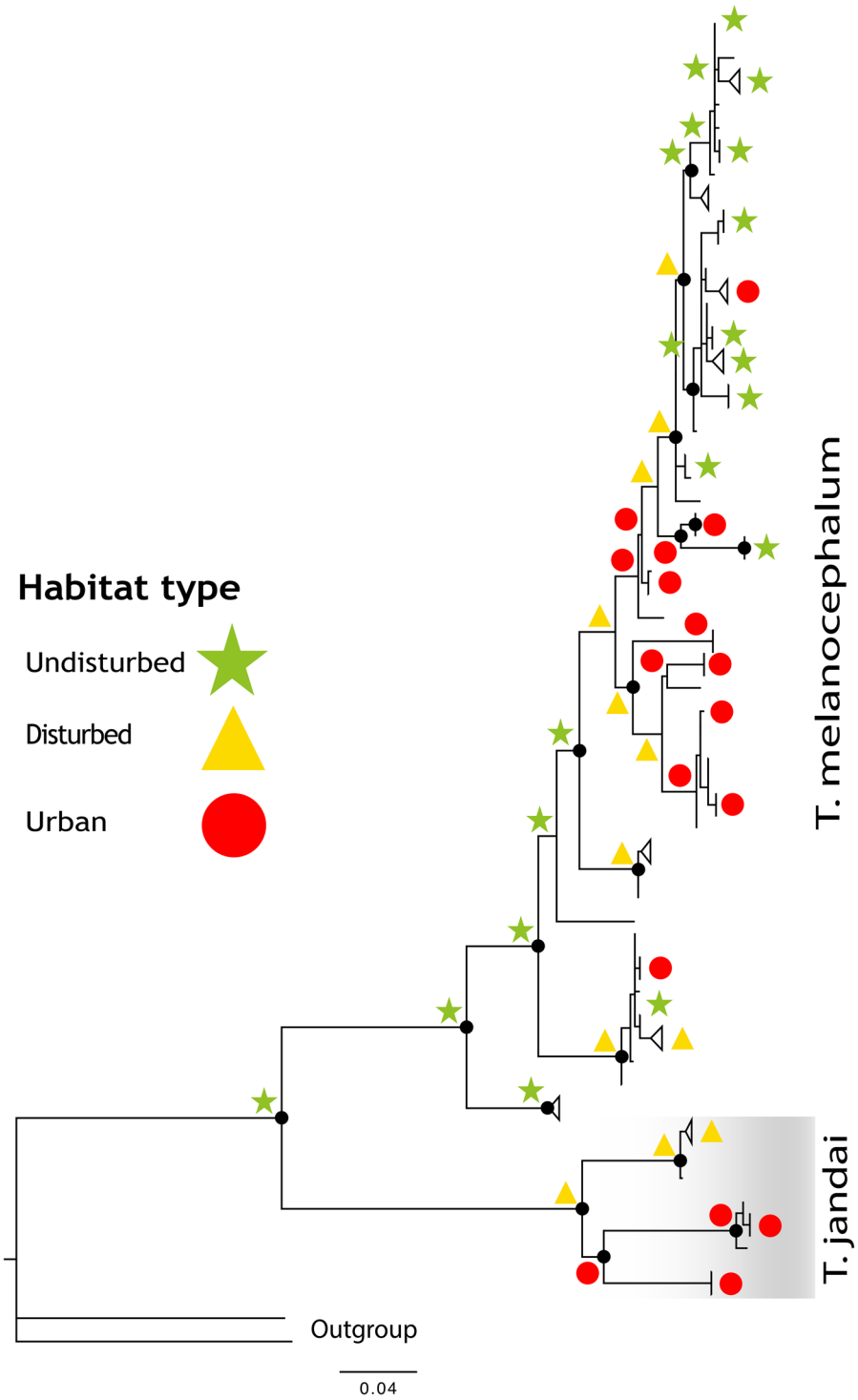

Fig. 5. Phylogenetic relationships among COI barcode sequences for *Tapinoma melanocephalum* and *T. jandai* inferred using IQ-TREE with the data partitioned by codon position. Some samples are collapsed for node ancestral states visualization (extended Fig. S7). The black circles on nodes indicate high support. Higher average values of BayesTraits analysis: q 1 0 (disturbed to undisturbed) = 1.223, q 0 2 (undisturbed to urban)= 1.638, q 1 2 (disturbed to urban)= 1.672, ancestral state in undisturbed habitat (mean: P 0 = 0.435), disturbed (mean: P 1 = 0.353) and urban (mean: P 2 = 0.212). The shaded clade represents *T. jandai*.

T. melanocephalum and the recently described *T. jandai* (Seifert 2025) under 2 approaches, one with SNPs from multilocus genomic data and the other with mitochondrial DNA data. This approach helped link the more robust genomic dataset with existing molecular databases to robustly delineate the 2 divergent lineages formerly treated as *T. melanocephalum*.

We recovered *Tapinoma* as monophyletic (Fig. 1) in accordance with previous studies (eg Ward et al. 2010, Moreau and

Table 4. Genetic characterization of *T. melanocephalum* and *T. jandai* populations

Region	Population	S	H	Hd	π
AUS/MEL/ORI	T_JANDAI	92	8	0.813	0.058
AFRICAN	COMOROS	1	2	0.428	0.006
AFRICAN	MADAGASCAR_1	66	5	0.763	0.044
AFRICAN	MADAGASCAR_2	44	2	0.20	0.013
AFRICAN	MAYOTTE	2	2	0.428	0.001
AUSTRALIAN	AUSTRALIA	56	5	0.893	0.036
MELANESIA	PNG_CENTRAL	26	6	0.893	0.016
MELANESIA	PNG_DARU	8	3	0.678	0.007
MELANESIA	PNG_MADANG	61	9	0.912	0.032
MELANESIA	PNG_MIANMIN	42	5	0.893	0.036
MELANESIA	PNG_PORT_MORESBY	53	6	0.928	0.036
MELANESIA	PNG_WANANG	7	5	0.818	0.003
MICRONESIA	MICRONESIA	42	3	0.524	0.018
NEARCTIC/PALAEARCTIC	NEARCTIC_PALAEARCTIC	1	1	0.005	0.001
NEOTROPICAL	SOUTH AMERICA	62	4	0.778	0.044
ORIENTAL	MALAYSIA	78	4	0.714	0.050
ORIENTAL	PALAU	85	5	0.786	0.051
POLYNESIA	FIJI	41	2	0.428	0.027
POLYNESIA	FRENCH_POLYNESIA	3	4	0.602	0.001
POLYNESIA	HAWAII	1	1	0.001	0.003

Segregating sites (S), number of haplotypes (h), haplotype diversity (Hd), and nucleotide diversity (π).

Bell 2013, Economo et al. 2018) and with *Aptinoma* as the sister group genus. However, given that we sampled only 13 of the 81 species in the genus, the validity of these topologies remains to be confirmed with more comprehensive taxon sampling. The principal clades in our phylogenetic reconstruction match with the groups proposed by Guerrero (2017), who delineated the *melanocephalum*, *sessile*, *ramulorum*, and *litorale* species groups.

There is overall congruence between the UCE and COI phylogenetic trees, with both supporting similar species boundaries. However, differences in taxon sets that we analyzed produced different crown group relationships among species. The analyses based on COI sequences alone cannot be considered adequate as standalone tools for inferring deeper phylogenetic relationships among most taxa (Rubinoff and Holland 2005, Dong et al. 2021) and thus we primarily focus on genomic results in this study.

The divergence times estimated for the crown-group origin of the genus in our study (49.4 to 34.4 Ma) (Fig. 2) were lower than some of the previously reported crown ages for *Tapinoma* (Moreau et al. 2006, Moreau and Bell 2013), but similar to divergence dates obtained by Economo et al. (2018) (46.6 Ma). Previous studies indicated a probable African origin of *Tapinoma* due to its phylogenetic relationship with *Aptinoma* (Wetterer 2009, Ward et al. 2010, Moreau and Bell 2013), although there is currently no fossil record that would support this hypothesis. Because the fossil *Tapinoma* in Canadian Hat Creek amber (52 Ma) has not been adequately documented (Ward et al. 2010), we used a soft minimum in our divergence time ranges. Our analyses suggested that the most recent common ancestor of *Tapinoma* lived in the Australasian (36.1%) or Oriental region (16.6%) (Fig. 2), dating to the middle Eocene.

Many lineages in our study originated in the Oriental and Australasian regions, followed by dispersal events into other regions. The principal *T. indicum* clade contains 2 separate African lineages, indicating that the African species originated from at least 2 diversifications. The presence of *T. litorale* and *T. ramulorum* in the same clade suggests an independent origin of these New World species from the other Palaearctic and Nearctic species (*T. madeirense* + *T. sessile*).

Most of the extant ant subfamilies expanded and diversified during the late Cretaceous to early Eocene (Grimaldi and Agosti 2000, Moreau et al. 2006, Ward et al. 2010). Our results revealed that the middle Eocene represents "dispersal-radiation time" for most *Tapinoma* lineages as well, and this may have been driven by the proliferation of angiosperms (Farrell 1998, Nelsen et al. 2023). Follow-up studies incorporating a broader representation of species from Africa and other regions are necessary for a more comprehensive understanding of the genus's biogeographic history and divergence dating. While our phylogenomic results are robust, the limited sampling may overlook key sister-group relationships, which could impact biogeographic interpretations and trait mapping.

Phylogeography and Biogeographic Origin of *T. melanocephalum*

Considering the importance and broad distribution of this synanthropic ant, it is useful to provide boundaries for the delimitation of this species. Guerrero (2018) redescribed *T. melanocephalum* and proposed characters for its discrimination from morphologically similar species (eg *T. atriceps*, *T. minutum*, *T. indicum*). Our phylogenetic analyses recovered *T. melanocephalum* + *T. jandai* as a sister group of *T. sessile* + *T. madeirense*, which confirmed their hypothesized relationship (Guerrero 2018). *T. indicum* and *T. minutum* are not closely related to *T. melanocephalum* and were recovered in 2 separate clades. However, most species-level relationships should be considered preliminary since we could not include some less common regional species.

The morphological forms of *T. melanocephalum* (*coronatum*, *malesianum*, *australis*) have been treated as subspecies that several authors described based on the morphological

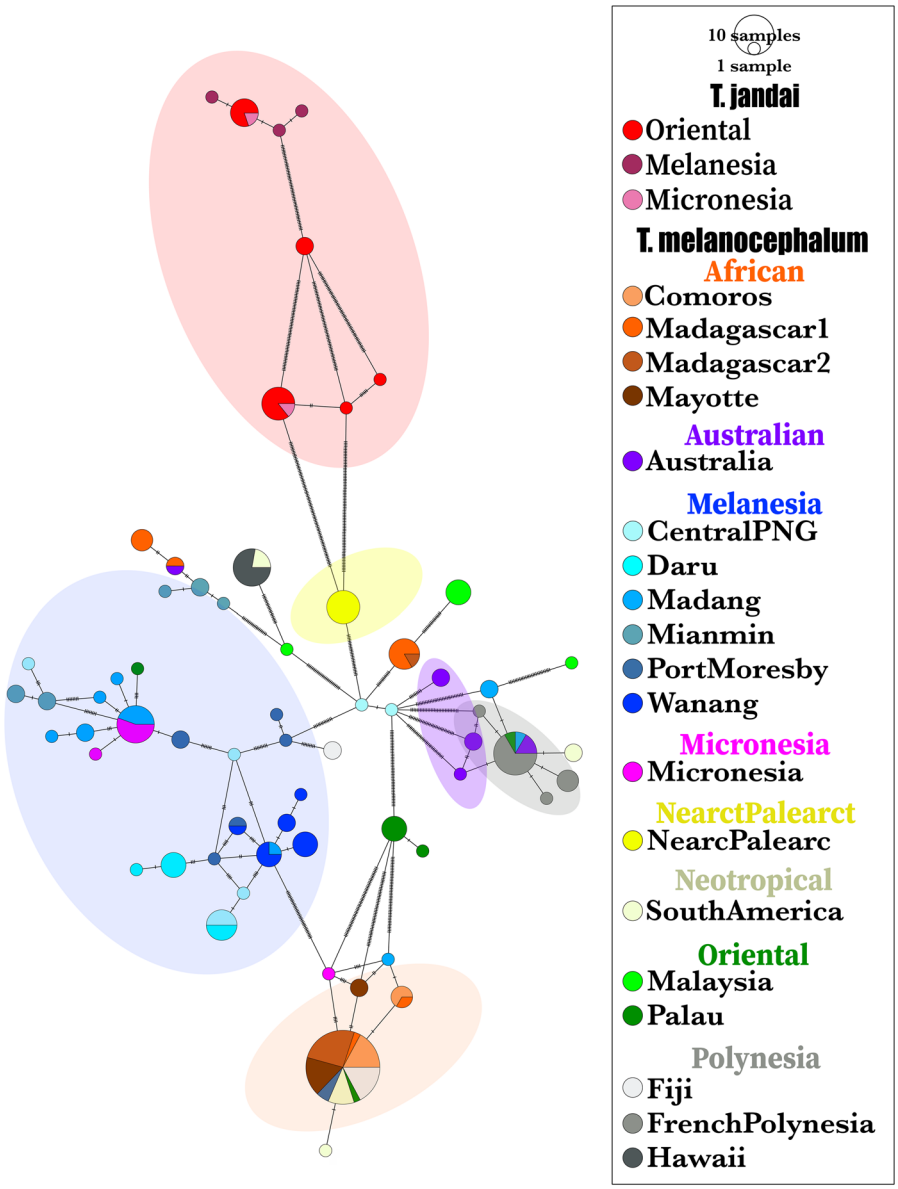

Fig. 6. Haplotype network. Median-joining network of samples of COI sequences for *Tapinoma melanocephalum* + *T. jandai*. Ellipse groups the populations by region; *T. jandai* = red, African = orange, Australasian = purple, Melanesia = blue, Nearctic/Palaearctic = yellow, Polynesia = gray.

Table 5. Statistics for Analysis of Molecular Variance (AMOVA) of haplotype variation of COI sequences between populations by biogeographic region (referred to as groups)

Source	d.f	Sum of square	Variance components	% variation
Between groups	8	2033.001	9.709 Va	40.01
Between populations within groups	11	708.493	6.167 Vb	25.41
Within populations	167	1401.591	8.393 Vc	34.58

variability of workers, especially evidenced in coloration and body shapes (eg vertex shape) (Forel 1908, 1913, Guerrero 2018). Seifert (2022) confirms that these subspecies are well allocated to *T. melanocephalum* (based on morphometric characters). With the same characters, he described *T. jandai* from populations originally assigned to *T. melanocephalum* from Asia (India, Pakistan, Oman, and Malaysia). Based on UCE (extracted SNPs) and COI markers, we confirm the distinction of the 2 species. Our vouchers and images from BOLD were morphologically distinct, exhibiting the difference in relative scape length noted by Seifert (2022, 2025). These morphological differences perfectly matched the 2 clades recognized with the molecular results. The species tree and structure results (both SNP-based analyses) showed a well-supported and clear pattern of differentiation between these 2 lineages (Fig. 3). Furthermore, species delimitation based solely on COI (mPTP and GMYC) (Fig. 4) recovered the same MOTUs as SNPs from UCEs for *T. melanocephalum* and *T. jandai*, with high intraspecific variation.

Within the *T. melanocephalum* SNPs tree (Fig. 3), we recovered one early divergent population from New Guinea (Australasian region) as a sister group of the remaining populations.

Then the next divergent population is from Palau (Oriental region). In the COI tree of *T. melanocephalum* and *T. jandai* (Fig. 5), the earliest divergent clade of *T. melanocephalum* is formed by samples from Palau. These clades are relevant for the reconstruction of the dispersal history of *T. melanocephalum* and for determining the ancestral region of the MRCA of *T. melanocephalum* in Australasia. The close phylogeographic relationship between New Guinea and Palau can be the result of common colonization patterns in Melanesian and Micronesian archipelagos, as has been documented in other ant groups and also plants (Rundell 2008, Matos-Maraví et al. 2018a, 2018b, Demeulenaere and Ickert-Bond 2022). Most flora and insect fauna on these archipelagos originated relatively recently, during the Miocene–Pleistocene (eg Clouse et al. 2015, Swenson et al. 2019). On the other hand, a recent colonization is possible and the sister group relationship to the remaining *T. melanocephalum* could result from high levels of population isolation or a bias of a single marker analysis.

The biogeographic reconstruction for both *T. melanocephalum* and *T. jandai* lineages is similar, suggesting the Australasian or Oriental origin with a divergence event in the late Miocene and Pliocene. Although an Australasian origin received higher probabilities than an Oriental origin in the biogeographic reconstruction, this could be a consequence of the taxon sampling in which samples from New Guinea and surrounding areas were overrepresented. Therefore, both an Australasian and Oriental origin of *T. melanocephalum* should be considered probable. While *T. melanocephalum* became widespread globally, *T. jandai* seems restricted mainly to the Indo-Oriental region. However, its occurrence in Oman (Seifert 2022, 2025) and anthropogenous introductions to temperate zones suggest a broader distribution.

Population Genetic Structure of *T. melanocephalum* and *T. jandai*

Our population genetic analyses of *T. melanocephalum* revealed a high haplotype diversity and low nucleotide diversity, with the neutrality tests significant in most populations ($P < 0.02$). This means that haplotypes are different in a reduced number of nucleotides with negative neutrality values, which suggests an abrupt demographic expansion process in a relatively recent time (Kaplan et al. 1988, Tajima 1989, Hamilton 2009), as also indicated by internal younger nodes in our estimated divergence times for the *T. melanocephalum* clade (Fig. 2).

Comparing genetic variation across geographic distances and biogeographic areas revealed an unbalanced genetic structuring, with some regions highly structured and others not. The low genetic differentiation may be attributed to the ghost ant's long-distance dispersals that frequently occur due to human activities (Seifert 2010), even among distant biogeographic regions (Fig. S5). In multiple cases, the populations (defined by locality) within one biogeographic region (referred to as groups in AMOVA) were highly differentiated from what might be expected from their geographic proximity or a single colonization event. An example of this pattern is high genetic differentiation between French Polynesia and Hawaii, Fiji and other surrounding regions, except Australia. Similarly, the 2 populations in Madagascar differ considerably in their genetic distances to other regions. Low genetic differentiation among South America and Fiji populations exhibits the opposite pattern.

The fact that some COI haplotypes are widely shared across multiple populations and biogeographic regions contributes to the relatively weak effect of distance on the genetic differentiation among the ghost ant populations. The shared haplotypes are evident in both the haplotype network (Fig. 6) and PCA analysis (Fig. S5), although most data are still structured mainly by the principal biogeographic regions. The *T. jandai* haplotypes were recovered well differentiated from the rest, with its haplotypes from China being close to a *T. melanocephalum* haplogroup from the Nearctic—Palaearctic region.

For *T. melanocephalum*, the most frequent haplotype in the African group is also the most broadly distributed one and shared by populations from other biogeographic regions. On the other hand, Melanesian haplogroups appear to be the most homogeneous, with few shared outside of the region, except for the coastal Madang region. Interestingly, the haplotypes found on the Palau archipelago are also highly diverse and related to Oriental, Melanesian, Nearctic, and African representatives, suggesting that species diversity on these islands resulted mainly from colonization from very diverse sources rather than local radiation, as found in other ants (Matos-Maraví et al. 2018a). To what extent these patterns reflect the actual genetic structure and to what extent they are affected by unequal and coincidental sampling efforts should be addressed in follow-up studies aiming for a balanced sampling across the regions and habitats.

Habitat Preferences in *T. melanocephalum*

Although *T. melanocephalum* is most commonly reported from disturbed, human-altered, and synanthropic habitats, it has also been found in undisturbed habitats worldwide, including primary forests (Wetterer 2009, Janda and Konecna 2011, Klimes et al. 2011). This raises the question of whether *T. melanocephalum* exhibits similar ecological roles and behaviors in both natural and disturbed habitats. Exploring this aspect could provide valuable information on whether the ecological behavior of the species depends on the habitat. For instance, studies in lowland dry forests of northern South America have reported very low abundances of this species compared to native ants, whereas in urban environments it can reach high densities (García-Avendaño and Guerrero 2018).

Mapping the habitat preferences of *T. melanocephalum* nests on the COI gene tree suggests a frequent unidirectional switch from primary and secondary vegetation (undisturbed or little disturbed areas) to synanthropic and disturbed habitats such as urban areas (Fig. 5). The tendency to inhabit and expand towards the urban environments is reflective of what the ghost ant is mainly known for: a widely distributed, synanthropic species which is opportunistically transported on a wide variety of household and commercial goods (Blumenfeld et al. 2022). A similar scenario was found in some species of *Nylanderia* Emery, 1906, and *Paratrechina longicornis* Latreille, 1802, where the ancestral switch in habitat preferences from undisturbed to disturbed or marginal habitats has been linked to increased dispersal capabilities and geographical range expansion (eg *Nylanderia bourbonica, N. vaga*, and *N. obscura*) (Matos-Maraví et al. 2018a).

Wong et al. (2023) consider *T. melanocephalum* a potential pest due to its extremely high environmental plasticity since it is one of the ant species most intercepted globally. These ecological strategies, along with an intranidal colony reproduction,

facilitate the dispersion and colonization around the world using anthropogenic routes (Smith 1965, Nickerson et al. 2004), leading to imbalanced genetic structure and globally widespread haplogroups as documented in our study. The pattern may be produced by fast spread and clonal reproduction that may lead to a supercolonial social structure. However, a detailed social and genetic structure analysis is needed to compare the gene flow and relationships among colonies.

Conclusion

We show that *Tapinoma* originated in the middle Eocene (49.4:34.4 Ma) in the Australasian or Oriental region and we report important dispersal-radiation events during the middle Miocene (about 30-00311 Ma). We confirm that the *T. melanocephalum* group consists of 2 lineages corresponding to 2 sister species that diverged about 13 Ma and originated in the Australasian or Oriental region. The population genetic structure of the ghost ant was unbalanced and heterogeneous, with little relation between genetic differentiation and geographic distance. The Melanesian haplogroups are the most differentiated from the rest, so it could be a population in the process of speciation within *T. melanocephalum*. The ecological shift of habitat preferences in *T. melanocephalum* could be linked to geographical range expansion, both natural and promoted by passive anthropogenous dispersal to urban environments. The simpler system of competitive relations between ants in urban environments coupled with the set of specific social structure traits of *T. melanocephalum* seem to contribute to its global colonization success. Further sampling and studies are needed to detail the colony genetic structure, genetic flow, and the history of the spread of this ubiquitous alien ant species.

Specimen collection statement

Nagoya Protocol: The authors attest that all legal and regulatory requirements, including export and import collection permits, have been followed for the collection of specimens from source populations at any international, national, regional, or other geographic level for all relevant field specimens collected as part of this study.

Acknowledgments

This paper is part of the requirements for obtaining a Doctoral degree at the Posgrado en Ciencias Biológicas, UNAM of O.P.F. The first author is grateful for the financial support received for his Ph.D. studies through the scholarship granted by the Consejo Nacional de Humanidades, Ciencias y Tecnologías (CONAHCyT), now renamed the Secretaría de Ciencia, Humanidades, Tecnología e Innovación (SECIHTI). We are very grateful the following colleagues who contributed specimens and data: H. Bharti, B. Blaimer, B.D. Blanchard, M. Borowiec, J. Czekanski-Moir, E.P. Economo, B.L. Fisher, P. Klimes, T. Ramage, and E. Sarnat. We thank R. Probst for help with extractions and UCE laboratory work, R. J. Guerrero for advice on the divergence time calibration, M. Quesada Avendaño and M. A. Villalda Quezada for support in the Laboratorio de Análisis y Síntesis Ecológica, UNAM, and A. González and A. Oceguera for advice on the project. We thank B. Seifert and 2 anonymous reviewers for considerably improving the earlier version of the manuscript. Computational resources were provided by the e-INFRA CZ project (ID: 90254), supported by the Ministry of Education, Youth and Sports of the Czech Republic.

Author Contributions

Oscar Pérez Flores (Conceptualization [lead], Data curation [equal], Formal analysis [lead], Investigation [lead], Methodology [lead], Validation [equal], Visualization [lead], Writing—original draft [lead], Writing—review & editing [lead]), Michael Branstetter (Data curation [equal], Funding acquisition [equal], Methodology [supporting], Writing—review & editing [supporting]), John Longino (Conceptualization [equal], Data curation [equal], Funding acquisition [equal], Investigation [equal], Methodology [equal], Validation [equal], Visualization [equal], Writing—review & editing [equal]), Pavel Matos-Maraví (Conceptualization [supporting], Data curation [supporting], Investigation [supporting], Methodology [supporting], Writing—review & editing [supporting]), Michaela Borovanska (Data curation [equal], Validation [equal], Writing—review & editing [supporting]), and Milan Janda (Conceptualization [equal], Data curation [equal], Funding acquisition [equal], Investigation [equal], Methodology [equal], Resources [equal], Validation [equal], Visualization [equal], Writing—review & editing [equal])

Supplementary Material

Supplementary material is available at *Insect Systematics and Diversity* online.

Funding

Funding was provided by Conahcyt DICB 282471 and UNAM PAPIIT N206818 (MJ), NSF grant DEB-1820839/DEB-2028284 (B. Blaimer), and DEB-1932405 (Ants of the World), and the Czech Science Foundation grant 22-35084J (PM-M). OP-F was supported by Posgrado en Ciencias Biológicas, UNAM, and the fellowship from CONAHCyT (2020-000013-01NACF-12930).

Conflicts of Interest

None declared.

References

Appel AG, Na JP, Lee CY. 2004. Temperature and humidity tolerances of the ghost ant, *Tapinoma melanocephalum* (Hymenoptera: Formicidae). *Sociobiology* 44:89–100.

Barden P. 2017. Fossil ants (Hymenoptera: Formicidae): ancient diversity and the rise of modern lineages. *Myrmecol. News* 24:1–30.

Blumenfeld AJ, Eyer PA, Helms AM, et al. 2022. Consistent signatures of urban adaptation in a native, urban invader ant *Tapinoma sessile*. *Mol. Ecol.* 31:4832–4850.

Bolger AM, Lohse M, Usadel B. 2014. Trimmomatic: a flexible trimmer for Illumina sequence data. *Bioinformatics* 30:2114–2120.

Bolton B. 1973. The ant genera of West Africa: a synonymic synopsis with keys (Hymenoptera: Formicidae). *Bull. Br Mus.* 27:319–366.

Bolton B. 2024. An Online Catalog of the Ants of the World [accessed 2024 Dec 19]. https://www.antcat.org/

Borowiec ML, Lee EK, Chiu JC, et al. 2015. Dissecting phylogenetic signal and accounting for bias in whole-genome datasets: a case study of the Metazoa. *BMC Genomics* 16:987.
Bouckaert RR. 2010. DensiTree: making sense of sets of phylogenetic trees. *Bioinformatics* 26:1372–1373.
Bouckaert RR, Heled J. 2014. DensiTree 2: seeing trees through the forest. bioRxiv 012401, preprint: not peer reviewed.
Bouckaert RR, Vaughan TG, Barido-Sottani J, et al. 2019. BEAST 2.5: an advanced software platform for Bayesian evolutionary analysis. *PLoS Comput. Biol.* 15:e1006650.
Branstetter MG, Longino JT, Ward PS, et al. 2017. Enriching the ant tree of life: enhanced UCE bait set for genome-scale phylogenetics of ants and other Hymenoptera. *Methods Ecol. Evol.* 8:768–776.
Brown Jr.. WL. 2000. Ants: standard methods for measuring and monitoring biodiversity. In: Agosti D, Majer JD, Alonso LE, Schultz TR, editors. *Diversity of ants*. Smithsonian Institution Press. p. 45–79.
Bryant D, Bouckaert R, Felsenstein J, et al. 2012. Inferring species trees directly from biallelic genetic markers: bypassing gene trees in a full coalescent analysis. *Mol. Biol. Evol.* 29:1917–1932.
Bustos X, Cherix D. 1998. Contribution to the biology of *Tapinoma melanocephalum* (Fabricius) (Hymenoptera: Formicidae). *Actes Coll. Insectes Soc.* 11:95–101.
Clouse RM, Janda M, Blanchard B, et al. 2015. Molecular phylogeny of Indo-Pacific carpenter ants (Hymenoptera: Formicidae, *Camponotus*) reveals waves of dispersal and colonization from diverse source areas. *Cladistics* 31:424–437.
Danecek P, Auton A, Abecasis G, et al. ; 1000 Genomes Project Analysis Group. 2011. The variant call format and VCFtools. *Bioinformatics* 27:2156–2158.
Demeulenaere E, Ickert-Bond SM. 2022. Origin and evolution of the Micronesian biota: insights from molecular phylogenies and biogeography reveal long-distance dispersal scenarios and founder-event speciation. *J. Sytemat. Evol.* 60:973–997.
Diniz-Filho JAF, Soares TN, Lima JS, et al. 2013. Mantel test in population genetics. *Genet. Mol. Biol.* 36:475–485.
Dlussky GM. 1999. New ants (hymenoptera, formicidae) from canadian amber. *Paleontol. J.* 33:409–412.
Dong Z, Wang Y, Li C, et al. 2021. Mitochondrial DNA as a molecular marker in insect ecology: current status and future prospects. *Ann. Entomol. Soc. Am.* 114:470–476.
Dray S, Dufour AB. 2007. The ade4 package: implementing the duality diagram for ecologists. *J. Stat. Soft.* 22:1–20.
Drummond AJ, Suchard MA, Xie D, et al. 2012. Bayesian phylogenetics with BEAUti and the BEAST 1.7. *Mol. Biol. Evol.* 29:1969–1973.
Economo EP, Narula N, Friedman NR, et al. 2018. Macroecology and macroevolution of the latitudinal diversity gradient in ants. *Nat. Comm.* 9:1778.
Escárraga ME, Lattke JE, Pie MR, et al. 2021. Morphological and genetic evidence supports the separation of two *Tapinoma* ants (Formicidae, Dolichoderinae) from the Atlantic Forest biome. *Zookeys* 1033:35–62.
Espadaler X, Espejo F. 2002. *Tapinoma melanocephalum* (Fabricius, 1793), a new exotic ant in Spain (Hymenoptera, Formicidae). *Orsis* 17:101–104.
Excoffier L, Lischer HE. 2010. Arlequin suite ver 3.5: a new series of programs to perform population genetics analyses under Linux and Windows. *Mol. Ecol. Resour.* 10:564–567.
Ezard T, Fujisawa T, Barraclough TG. 2009. SPLITS: SPecies' LImits by Threshold Statistics. R package version 1.0-18/r45 [accessed 2024 Sep 20]. http://R-Forge.R-project.org/projects/splits/
Faircloth BC. 2013. Illumiprocessor: a trimmomatic wrapper for parallel adapter and quality trimming [accessed 2024 Jun 12]. http://dx.doi.org/10.6079/J9ILL
Faircloth BC. 2016. PHYLUCE is a software package for the analysis of conserved genomic loci. *Bioinformatics* 32:786–788.
Farrell BD. 1998. " Inordinate Fondness" explained: why are there so many beetles?.*Science* 281:555–559.
Foerster A. 1950. *Hymenopterologische studien*. 1. Formicariae. Ernst Ter Meer.
Forel A. 1908. Fourmis de Costa-Rica récoltées par M. *Paul Biolley. Bull. Soc. Vaudoise Sci. Nat.* 44:35–72.
Forel A. 1913. Wissenschaftliche Ergebnisse einer Forschungsreise nach Ostindien ausgefu¨hrt im Auftrage der Kgl. Preuss. Akademie der Wissenschaften zu Berlin von H. v. Buttel-Reepen. II. Ameisen aus Sumatra, Java, Malacca und Ceylon. Gesammelt von Herrn Prof. Dr v. Buttel-Reepen in den Jahren 1911-1912. Zool. Jahrb. *Abt. Anat. Ontog. Tiere*. 36:1–148.
Fowler HG, Bueno OC, Sadatsune T, et al. 1993. Ants as potential vectors of pathogens in hospitals in the state of São Paulo, Brazil. *Int. J. Trop. Insect Sci.* 14:367–370.
García-Avendaño EI, Guerrero RJ. 2018. Taxonomía y distribución de las hormigas del género *Tapinoma* (Formicidae: Dolichoderinae) en Colombia. *Rev. Colomb. Entomol.* 44:223–237.
Greenberg L, Rust MK, Klotz JH, et al. 2010. Impact of ant control technologies on insecticide runoff and efficacy. *Pest Manag. Sci.* 66:980–987.
Grimaldi D, Agosti D. 2000. A formicine in New Jersey Cretaceous amber (Hymenoptera: Formicidae) and early evolution of the ants. *Proc. Natl. Acad. Sci. U S A* 97:13678–13683.
Guerrero RJ. 2017. Revisión taxonómica de las hormigas *Tapinoma* Fôrster (Hymenoptera: Formicidae: Dolichoderinae) en la reión neotropical [doctoral dissertation]. Central University of Venezuela.
Guerrero RJ. 2018. Taxonomic identity of the ghost ant, *Tapinoma melanocephalum* (Fabricius, 1793) (Formicidae: Dolichoderinae). *Zootaxa* 4410:497–510.
Guerrero RJ. 2021. Transfer of two South American ant species from *Tapinoma* Foerster, 1850 to *Forelius* Emery, 1888 (Hymenoptera: Formicidae: Dolichoderinae). *Zootaxa* 4920:zootaxa.4920.3.8.
Guindon S, Dufayard JF, Lefort V, et al. 2010. New algorithms and methods to estimate maximum-likelihood phylogenies: assessing the performance of PhyML 3.0. *Syst. Biol.* 59:307–321.
Hamilton MB. 2009. *Population genetics*. Wiley-Blackwell.
Harris RS. 2007. Improved pairwise alignment of genomic DNA [PhD thesis]. Pennsylvania State University.
Hoang DT, Chernomor O, Von Haeseler A, et al. 2018. UFBoot2: improving the ultrafast bootstrap approximation. *Mol. Biol. Evol.* 35:518–522.
Janda M, Konecna M. 2011. Canopy assemblages of ants in a New Guinea rain forest. *J. Trop. Ecol.* 27:83–91.
Janicki J, Narula N, Ziegler M, et al. 2016. Visualising and interacting with large-volume biodiversity data using client–server web-mapping applications: the design and implementation of antmaps.org. *Ecol. Inform.* 32:185–193.
Jombart T. 2008. adegenet: a R package for the multivariate analysis of genetic markers. *Bioinformatics* 24:1403–1405.
Jombart T, Devillard S, Balloux F. 2010. Discriminant analysis of principal components: a new method for the analysis of genetically structured populations. *BMC Genet.* 11:94–15.
Kaplan NL, Darden T, Hudson RR. 1988. The coalescent process in models with selection. *Genetics* 120:819–829.
Kapli P, Lutteropp S, Zhang J, et al. 2017. Multi-rate Poisson tree processes for single-locus species delimitation under maximum likelihood and Markov chain Monte Carlo. *Bioinformatics* 33:1630–1638.
Kass JM, Guénard B, Dudley KL, et al. 2022. The global distribution of known and undiscovered ant biodiversity. *Sci. Adv.* 8:eabp9908.
Katoh K, Standley DM. 2013. MAFFT multiple sequence alignment software version 7: improvements in performance and usability. *Mol. Biol. Evol.* 30:772–780.
Klimes P, Janda M, Ibalim S, et al. 2011. Experimental suppression of ants foraging on rainforest vegetation in New Guinea: testing methods for a whole-forest manipulation of insect communities. *Ecol. Entomol.* 36:94–103.
Lanfear R, Calcott B, Ho SY, et al. 2012. PartitionFinder: combined selection of partitioning schemes and substitution models for phylogenetic analyses. *Mol. Biol. Evol.* 29:1695–1701.

Lanfear R, Frandsen PB, Wright AM, et al. 2017. PartitionFinder 2: new methods for selecting partitioned models of evolution for molecular and morphological phylogenetic analyses. *Mol. Biol. Evol.* 34:772–773.

LaPolla JS, Brady SG, Shattuck SO. 2010. Phylogeny and taxonomy of the *Prenolepis* genus-group of ants (Hymenoptera: Formicidae). *Syst. Entomol.* 35:118–131.

Leigh JW, Bryant D. 2015. POPART: 2015. Full-feature software for haplotype network construction. *Methods Ecol. Evol.* 6:1110–1116.

Li H. 2013. Aligning sequence reads, clone sequences and assembly contigs with BWA-MEM. arXiv 1303.3997, preprint: not peer reviewed.

Li H, Durbin R. 2010. Fast and accurate long-read alignment with Burrows–Wheeler transform. *Bioinformatics* 26:589–595.

Li H, Handsaker B, Wysoker A, et al. ; 1000 Genome Project Data Processing Subgroup. 2009. The sequence alignment/map format and SAMtools. *Bioinformatics* 25:2078–2079.

Lischer HE, Excoffier L. 2012. PGDSpider: an automated data conversion tool for connecting population genetics and genomics programs. *Bioinformatics* 28:298–299.

Luo YP, Chang NT. 2013. Strategies for controlling the ghost ant, *Tapinoma melanocephalum* (Hymenoptera: Formicidae) with liquid bait. *J. Asia-Pac. Entomol.* 16:113–118.

Maddison WP, Maddison DR. 2018. Mesquite: a modular system for evolutionary analysis. Version 3.5 [accessed 2024 Jul 12]. https://www.mesquiteproject.org/.

Matos-Maraví P, Clouse RM, Sarnat EM, et al. 2018a. An ant genus-group (*Prenolepis*) illuminates the biogeography and drivers of insect diversification in the Indo-Pacific. *Mol. Phylogenet. Evol.* 123:16–25.

Matos-Maraví P, Matzke NJ, Larabee FJ, et al. 2018b. Taxon cycle predictions supported by model-based inference in Indo-Pacific trap-jaw ants (Hymenoptera: Formicidae: Odontomachus). *Mol. Ecol.* 27:4090–4107.

Matzke NJ. 2012. Founder-event speciation in BioGeoBEARS package dramatically improves likelihoods and alters parameter inference in dispersal-extinction-cladogenesis (DEC) analyses. *Front. Biogeogr.* 4:210.

Matzke NJ. 2013. BioGeoBEARS: BioGeography with Bayesian (and likelihood) evolutionary analysis in R Scripts. R Package, version 0.2.1 [accessed 2024 Sep 15] http://CRAN.R-project.org/package=BioGeoBEARS

McKenna A, Hanna M, Banks E, et al. 2010. The Genome Analysis Toolkit: a MapReduce framework for analysing next-generation DNA sequencing data. *Genome Res.* 20:1297–1303.

Minh BQ, Nguyen MAT, von Haeseler A. 2013. Ultrafast approximation for phylogenetic bootstrap. *Mol. Biol. Evol.* 30:1188–1195.

Minh BQ, Schmidt HA, Chernomor O, et al. 2020. IQ-TREE 2: new models and efficient methods for phylogenetic inference in the genomic era. *Mol. Biol. Evol.* 37:1530–1534.

Moreira D, Morais VD, Vieira-da-Motta O, et al. 2005. Ants as carriers of antibiotic-resistant bacteria in hospitals. *Neotrop. Entomol.* 34:999–1006.

Moreau CS, Bell CD. 2013. Testing the museum versus cradle tropical biological diversity hypothesis: phylogeny, diversification, and ancestral biogeographic range evolution of the ants. *Evolution* 67:2240–2257.

Moreau CS, Bell CD, Vila R, et al. 2006. Phylogeny of the ants: diversification in the age of angiosperms. *Science* 312:101–104.

Nelsen MP, Moreau CS, Boyce CK, et al. 2023. Macroecological diversification of ants is linked to angiosperm evolution. *Evol. Lett.* 7:79–87.

Nickerson JC, Bloomcamp CL, Fasulo TR. 2004. *Ghost ant, Tapinoma melanocephalum (fabricius) (insecta: Hymenoptera: Formicidae)*. University of Florida EDIS.

Nurk S, Meleshko D, Korobeynikov A, et al. 2017. metaSPAdes: a new versatile metagenomic assembler. *Genome Res.* 27:824–834.

Pagel M, Meade A. 2017. BayesTraits V3.0 [accessed 2024 Jul 12] http://www.evolution.rdg.ac.uk/BayesTraitsV3/BayesTraitsV3.html

Peakall R, Smouse PE. 2012. GenAlEx 6.5: genetic analysis in Excel. Population genetic software for teaching and research—an update. *Bioinformatics* 28:2537–2539.

Perkovsky EE, Rasnitsyn AP, Vlaskin AP, et al. 2007. A comparative analysis of the Baltic and Rovno amber arthropod faunas: representative samples. *Afr. Invertebr.* 48:229–245.

Pons J, Barraclough TG, Gomez-Zurita J, et al. 2006. Sequence based species delimitation for the DNA taxonomy of undescribed insects. *Syst. Biol.* 55:595–609.

Pritchard JK, Stephens M, Donnelly P. 2000. Inference of population structure using multilocus genotype data. *Genetics* 155:945–959.

R Core Team. 2020. *R: A Language and Environment for Statistical Computing*. R Foundation for Statistical Computing. https://www.R-project.org

Rambaut A, Drummond AJ, Xie D, et al. 2018. Posterior summarisation in Bayesian Phylogenetics using Tracer 1.7. *Syst. Biol.* 67:901–904.

Ratnasingham S, Hebert PD. 2007. BOLD: the Barcode of Life Data System (http://www.barcodinglife.org). *Mol. Ecol. Notes.* 7:355–364.

Rozas J, Ferrer-Mata A, Sánchez-DelBarrio JC, et al. 2017. DnaSP 6: DNA sequence polymorphism analysis of large data sets. *Mol. Biol. Evol.* 34:3299–3302.

Rubinoff D, Holland BS. 2005. Between two extremes: mitochondrial DNA is neither the panacea nor the nemesis of phylogenetic and taxonomic inference. *Syst. Biol.* 54:952–961.

Rundell RJ. 2008. Cryptic diversity, molecular phylogeny and biogeography of the rock-and leaf litter-dwelling land snails of Belau (Republic of Palau. *Philos. Trans. R Soc. Lond. B Biol. Sci.* 363:3401–3412.

Seifert B. 2010. Intranidal mating, gyne polymorphism, polygyny, and supercoloniality as factors for sympatric and parapatric speciation in ants. *Ecol. Entomol.* 35:33–40.

Seifert B. 2012. Clarifying naming and identification of the outdoor species of the ant genus *Tapinoma* FÖRSTER, 1850 (Hymenoptera: Formicidae) in Europe north of the Mediterranean region with description of a new species. *Myrmecol. News* 16:139–147.

Seifert B. 2022. The previous concept of the cosmopolitan pest ant *Tapinoma melanocephalum* (FABRICIUS, 1793) includes two species (Hymenoptera: Formicidae: *Tapinoma*). *Osmia* 10:35–44.

Seifert B. 2025. Treachery pigmentation pattern leads to misidentification: *Tapinoma melanocephalum* (Fabricius), *Tapinoma pygmaeum* (Dufour) and *Tapinoma jandai* sp. nov. (Hymenoptera, Formicidae). *CTE*. 75:245–252.

Seifert B, Kaufmann B, Fraysse L. 2024. A taxonomic revision of the Palaearctic species of the ant genus *Tapinoma* Mayr 1861 (Hymenoptera: Formicidae). *Zootaxa* 5435:1–74.

Shattuck SO. 1992. Generic revision of the ant subfamily Dolichoderinae (Hymenoptera: Formicidae). *Sociobiology* 21:1–181.

Smith EH, Whitman RC. 1992. *NPMA field guide to structural pests*. Natural Pest Control Association. p. 800.

Smith MR. 1965. House-infesting ants of the eastern United States. Their recognition, biology, and economic importance. *US. Dept. Agric. Technol. Bull.* 1326:1–105.

Swenson U, Havran JC, Munzinger J, et al. 2019. Metapopulation vicariance, age of island taxa and dispersal: a case study using the Pacific plant genus *Planchonella* (Sapotaceae). *Syst. Biol.* 68:1020–1033.

Tagliacollo VA, Lanfear R. 2018. Estimating improved partitioning schemes for ultraconserved elements. *Mol. Biol. Evol.* 35:1798–1811.

Tajima F. 1989. Statistical method for testing the neutral mutation hypothesis by DNA polymorphism. *Genetics* 123:585–595.

Talavera G, Castresana J. 2007. Improvement of phylogenies after removing divergent and ambiguously aligned blocks from protein sequence alignments. *Syst. Biol.* 56:564–577.

Venkataramaiah GH, Rehman PA. 1989. Ants associated with the mealybugs of coffee. *Indian Coffee* 43:13–14.

Ward PS. 2010. Ant ecology. In: Lach L, Parr CL, Abbott KL, editors. *Taxonomy, phylogenetics, and evolution*. Oxford University Press. p. 3–17.

Ward PS, Brady SG, Fisher BL, et al. 2010. Phylogeny and biogeography of dolichoderine ants: effects of data partitioning and relict taxa on historical inference. *Syst. Biol.* 59:342–362.

Wetterer JK. 2009. Worldwide spread of the ghost ant, *Tapinoma melanocephalum* (Hymenoptera: Formicidae). *Myrmecol. News* 12:23–33.

Wheeler WM. 1922. Ants of the American Museum Congo expedition. A contribution to the myrmecology of Africa. VII. Keys to the genera and subgenera of ants. *Bull. Am. Mus. Nat. Hist.* 45: 631–710.

Wilson EO. 1967. The ants of Polynesia (Hymenoptera: Formicidae). *Annu. Rev. Ecol. Syst.* 33:181–233.

Wong MK, Economo EP, Guénard B. 2023. The global spread and invasion capacities of alien ants. *Curr. Biol.* 33:566–571.e3.

Zhang J, Kapli P, Pavlidis P, et al. 2013. A general species delimitation method with applications to phylogenetic placements. *Bioinformatics* 29:2869–2876.

Zhang C, Sayyari E, Mirarab S. 2017. RECOMB-CG comparative genomics. In: Meidanis J, Nakhleh L, editors. *ASTRAL-III: increased scalability and impacts of contracting low support branches*. Springer. p. 53–75.

Zheng C, Yang F, Zeng L, et al. 2018. Genetic diversity and colony structure of *Tapinoma melanocephalum* on the islands and mainland of South China. *Ecol. Evol.* 8:5427–5440.